

First-principles study of DX centers in CdTe, ZnTe, and $Cd_xZn_{1-x}Te$ alloys

C. H. Park and D. J. Chadi

NEC Research Institute, 4 Independence Way, Princeton, New Jersey 08540

(Received 7 February 1995)

Large lattice relaxation models for DX centers in CdTe, ZnTe, and $Cd_xZn_{1-x}Te$ alloys are examined through first-principles pseudopotential calculations. The calculated binding energies of DX centers for Al, Ga, In, Cl, Br, and I donor impurities in CdTe and their pressure and alloy dependence in $Cd_xZn_{1-x}Te$ are in good agreement with experimental data. Three distinct types of DX -like structures characterized by either bond rupture or bond compression are found for column VII donors. The relative stability of these structures is impurity and pressure dependent.

I. INTRODUCTION

There is now considerable experimental evidence in support of self-compensating defect formation in n -type CdTe-based alloys such as $Cd_xMg_{1-x}Te$,^{1,2} $Cd_xZn_{1-x}Te$,^{3,4} and $Cd_xMn_{1-x}Te$.^{1,5} The self-compensation centers prevent the achievement of high carrier densities through doping.^{6,7} We show in this paper that the observed doping limits and self-compensation center in II-VI semiconductors can be explained by the formation of DX centers which for column III (but not always for column VII) impurities are similar to those of the well-known DX centers in III-V alloys particularly in the $Al_xGa_{1-x}As$ system.⁸ We find that for the case of a Ga impurity the DX level actually lies below the conduction-band minimum in CdTe and ZnTe.

The conversion of the shallow hydrogenic donor into a deep relaxed one can be achieved by adding Zn, Mn, or Mg to CdTe.¹⁻⁵ As in GaAs, hydrostatic pressure leads to a shallow-deep conversion of donor levels in n -type CdTe.⁹ The most important experimental observation indicating the presence of DX centers is persistent photoconductivity (PPC), which arises from bistability of the impurity, and which is accompanied by a persistent electron paramagnetic resonance (EPR) signal.⁴ The large Stokes shift between the thermal and optical ionization energies is indicative of a large lattice relaxation.

Among many models suggested to explain the DX center in III-V and II-VI semiconductors,¹⁰⁻¹³ the "negative- U " broken-bond geometry is the most successful microscopic model.¹⁰ It was initially applied to explain the DX centers in Si-doped $Al_xGa_{1-x}As$ alloys. The model explains the self-compensation phenomenon, the PPC effect, and the large Stokes shift between the thermal and optical ionization energies of DX centers. According to the negative- U model, when a donor atom captures an electron, the total energy is reduced by bond breaking. The resulting two dangling bonds are generally fully occupied, making the two atoms with broken bonds chemically inert, thereby leading to a barrier against re-bonding. The absence of an EPR signal and persistent photoconductivity are satisfactorily explained by this model.

In this paper we examine in detail the broken-bond and other geometries for DX centers in CdTe and $Cd_xZn_{1-x}Te$ semiconductors, and calculate the pressure dependence of binding energies in CdTe. We find that although the ionic displacements leading to DX formation for column VII impurities in CdTe have C_{3v} symmetry, they are not always of the bond-breaking type.

The paper is organized as follows. In Sec. II we describe the method of calculation. The results of the total-energy calculations for the binding energies of DX centers and their pressure dependence in CdTe for column III donors are discussed in Sec. III A. In Sec. III B we extend the results to DX centers arising from column VII impurities. The conclusions from our study are presented in Sec. IV.

II. METHOD OF CALCULATION

We use the first-principles pseudopotential total-energy¹⁴ method within the local density functional approximation¹⁵ (LDA) in momentum space.¹⁶ Norm-conserving nonlocal soft pseudopotentials are generated by the scheme proposed by Troullier and Martins¹⁷ and the Kleinman-Bylander type of fully separable pseudopotentials¹⁸ are constructed. Semirelativistic corrections to the ionic pseudopotentials are included.¹⁹ The Ceperly-Alder correlation as parametrized by Perdew and Zunger is used.²⁰

The stability of the negative- U large lattice relaxation model is examined by considering the following reaction:



where d denotes a substitutional impurity as in Fig. 1(a), and DX denotes the broken-bond geometry shown in Fig. 1(b) for a column III impurity, and the superscripts denote the corresponding charge states. Since both the left- and right-hand sides are charge neutral, this reaction is independent of the Fermi level.

We include the localized d orbitals for column II elements (i.e., Cd or Zn) in our pseudopotential calculations using a 16-atom fcc cell. Since the localized d potential requires a high cutoff energy for plane-wave expansions and an extremely large CPU time, we did not perform

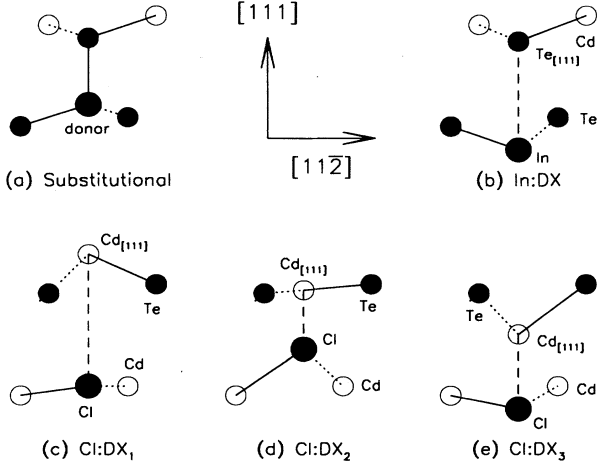


FIG. 1. Schematic atomic configurations of donors on a (110) plane for (a) shallow donor, (b) large lattice relaxation geometry for column III donor, and (c) DX_1 , (d) DX_2 , and (e) DX_3 structures with large lattice relaxations for column VII donors. Dotted lines denote bonds not on the (110) plane.

these full scale calculations for a larger cell. However, atomic relaxations in the larger 64-atom cell were estimated (using a partial-core-corrected pseudopotential²¹ to avoid the use of localized d orbitals) and found to increase the binding energies of the DX centers by 0.12 and 0.10 eV for the In and Cl donors, respectively. The atomic coordinates obtained from the two types of pseudopotentials are very close to each other. By comparing the 16-atom cell calculations for both types of pseudopotentials, we could estimate the size of the error in the calculated binding energies when partial core corrections, instead of localized d states, are used. These errors are about 0.16 and 0.12 eV for In and Cl donors, respectively.

In calculations for other donors, we used a 32-atom cell and partial-core-corrected pseudopotentials for column II elements, and we then made corrections for the small errors caused by the use of partial core corrections. After testing many types of k -point samplings, to do the Brillouin zone summation, we use five special k points for a 16-atom supercell, and four k points for the 32-atom bcc supercell. The error from these k -point sets and supercells is estimated to be within 0.1 eV. When localized d states are included, a kinetic energy cutoff of 40 Ry is used for the plane-wave expansion, while we use a

12-Ry cutoff for partial-core-corrected pseudopotentials.

To test the accuracy of the pseudopotentials, we have examined the ground-state properties of CdTe and ZnTe and the results are shown in Table I. The structural properties are well reproduced by both types of potentials. The calculated energy gaps are underestimated by about 1.0 eV, consistent with other calculations using the local density approximation.

The $Cd_xZn_{1-x}Te$ alloys are simulated by using the virtual crystal approximation (VCA). The VCA approach has been successfully applied to predict the stability of DX centers in Si-doped $Al_xGa_{1-x}As$ alloys.²²

III. RESULTS

A. Column III donors

For column III donors such as In, Ga, and Al in CdTe, the microscopic structure of the negative- U large lattice relaxation geometry is similar to that of DX centers in III-V semiconductors. The DX state leads to a broken-bond geometry with trigonally C_{3v} symmetry, i.e., one of the four donor- $Te_{[111]}$ bonds along [111] direction is broken. For example, an In impurity atom is displaced by 1.89 Å along the $[\bar{1}\bar{1}\bar{1}]$ direction into an “interstitial” position as shown in Fig. 1(b). The resulting threefold coordinated $Te_{[111]}$ atom is slightly displaced by 0.15 Å along the $[\bar{1}\bar{1}\bar{1}]$ axis. The separation between the In and $Te_{[111]}$ atoms is calculated to be 4.54 Å, while the other three unbroken donor-Te bond lengths are 3.04 Å, close to the 3.14-Å value in the tetrahedral substitutional d^+ state. These bonds make an angle of 69.0° with the [111] axial direction.

A fourfold coordinated structure (the D^- center) with T_d symmetry, accompanied by a breathing mode relaxation, is also available for a negatively charged state, but the D^- state does not give a deep state, and there is no barrier between the D^- and the shallow donor d^0 states. The binding energy of the D^- state is generally insensitive to pressure or composition ratio x . In this paper, we concentrate on the trigonally symmetric state, which undergoes a larger lattice relaxation.

The electronic charge density contours of the midgap DX level for the broken-bond geometry of an In donor in CdTe are shown in Fig. 2. The charge density is strongly localized around the $Te_{[111]}$ atom and the antibonding region of the donor atom, similar to the case of the Si: DX center in GaAs.^{10,23} The energy levels of the localized state are located 0.55, 0.61, and 0.54 eV below the

TABLE I. The lattice constant a_0 , bulk modulus B , and energy gap E_g (eV) [and its pressure derivatives (meV/kbar) in parentheses] are calculated with both partial-core-corrected pseudopotentials (PCPP) and with localized d -orbital included pseudopotentials (DPP), and the results are compared with experimental data (Ref. 20) for CdTe and ZnTe.

	CdTe			ZnTe		
	a_0 (Å)	B (GPa)	E_g (dE_g/dP)	a_0 (Å)	B (GPa)	E_g (dE_g/dP)
PCPP	6.38	0.50	0.78 (6.6)	6.10	0.49	1.27
DPP	6.43	0.45	0.46 (6.2)	6.06	0.53	0.94
Experiment	6.48		1.60 (8.0)	6.10		2.39

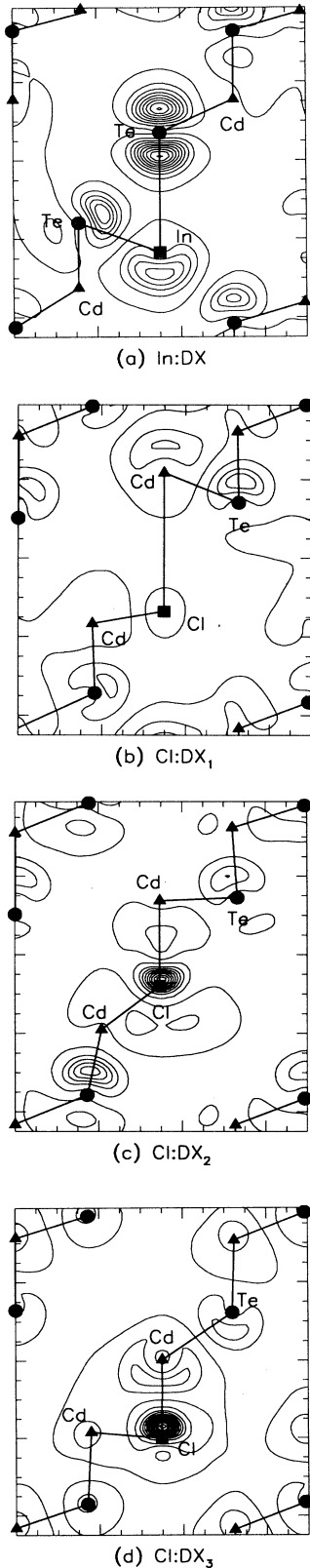


FIG. 2. Charge density contours are plotted in a (110) plane of CdTe for (a) In DX state, and for (b) DX_1 , (c) DX_2 , and (d) DX_3 states of a Cl donor. The contour spacings are chosen to be five electrons per cell volume. The cell volume is 1008.9 \AA^3 .

conduction-band minimum for Al, Ga, and In donors, respectively, in CdTe.

For Al: DX in CdTe, the binding energy of the broken-bond geometry is calculated to be -0.42 [i.e., the reaction in Eq. (1) is endothermic by 0.42 eV]. For Ga, the binding energy is $+0.08$ (i.e., the DX state is more stable than the shallow donor state), and for In it is -0.04 eV . The binding energies for $\text{Cd}_{0.5}\text{Zn}_{0.5}\text{Te}$ and ZnTe are shown in Fig. 3 and in Table II. Among the three donor impurities, Al gives the most stable shallow donor state.

As the donor impurity concentration increases, the energy level of the free electrons in the conduction band increases, and DX -like states become more stable than d^0 at sufficiently heavy doping. Thus the doping limit of CdTe can be estimated from the calculated resonance energy of the DX center with respect to the conduction band. The doping limits for In and Al impurities in CdTe are estimated to occur at about 1.8×10^{18} and $6.1 \times 10^{19} \text{ cm}^{-3}$, respectively. The value for In is in good agreement with the experimental observation⁶ that the highest measured electron concentration obtained from In doping in CdTe is $1.3 \times 10^{18} \text{ cm}^{-3}$. Our results suggest that Al doping should give a higher free electron concentration.

An important test of the proposed structures for DX centers is provided by a comparison of the theoretical pressure coefficients of the binding energies with experimental data. The theoretical results for column III impurities in CdTe are shown in Fig. 4. It is found that pressure stabilizes the DX centers with respect to the shallow donor states. A similar behavior was found in previous calculations for DX centers in III-V semiconductors.^{22,24} The shallow-deep transitions are estimated to occur at pressures of about 5 and 41 kbar for In and Al donors, respectively. The pressure derivatives of the DX binding energies are calculated to be 10.4, 10.4, and 9.4 meV/kbar for In, Al, and Ga donors, respectively. The pressure variations are nearly the same for all three column III donors, independent of their binding energies at zero pressure.

Our results are in good agreement with experimental data. Iseler *et al.*⁹ observed an increase of resistivity with pressure for n -type CdTe, which reflects the generation of deep states or a shallow-deep transition at a pressure of about 6–12 kbar for In, depending on the electron

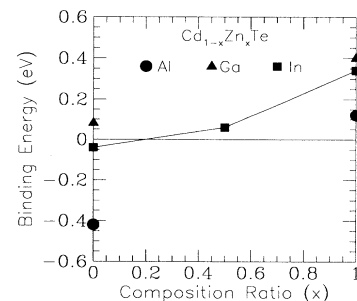


FIG. 3. The binding energies of DX centers of the column III donors In, Ga, and Al in CdTe, ZnTe, and $\text{Cd}_{1-x}\text{Zn}_x\text{Te}$ alloys. The DX center is more stable than the shallow donor state for all three donors in ZnTe.

TABLE II. The binding energies in eV of *DX* centers for Ga, Al, and In donors in CdTe and ZnTe. Negative values indicate that the shallow donor state is more stable than the *DX* center.

	Ga	Al	In
CdTe	0.08	-0.42	-0.04
ZnTe	0.40	0.12	0.34

carrier density. For Al, the transition was not observed. They estimated that the pressure derivatives of the energy levels of non-effective-mass donors for column III donors are about 18 meV/kbar,⁹ assuming that electrons are captured in a non- Γ -like state resonant in the conduction band. It was noted, however, that if the donors are assumed to be compensated by acceptors, the pressure derivatives of acceptor levels should be divided by 2,⁹ which gives a pressure coefficient of 9 meV/kbar. Foyt, Halsted, and Paul obtained a pressure derivative of 12.6 meV/kbar by assuming the latter.²⁵ These values are close to our results, and negative-*U* *DX* centers can now be understood to play the role of acceptors.

The shallow-deep transition with pressure can be explained by the increase in energy of the conduction-band edge. The energy level of the shallow donor state follows the conduction band, while the *DX* level is relatively insensitive to pressure. Thus the pressure stabilizes the *DX* state. The pressure derivative of the *band gap* at Γ is calculated to be 6.2 meV/kbar, which is *smaller* than the various *DX* binding energies. The explanation for this is that the *DX* state has atomlike character and is insensitive to pressure while the energies of the valence-band maximum and the conduction-band edge both go up with pressure.

In ZnTe, the atomic structure of the *DX* center is predicted to be similar to that in CdTe. The *DX* binding energies in ZnTe are calculated to be 0.12, 0.40, and 0.34 eV for Al, Ga, and In donors, respectively, i.e., all three *DX* centers are stable with respect to the shallow donor states. The *DX* binding energies in ZnTe are about 0.4 eV larger than those in CdTe. Since the valence-band

maximum (VBM) state consists mainly of the *p* orbitals of Te atoms in both CdTe and ZnTe, the VBM offset between the two is small. In addition, the nearest-neighbor atomic environments of column III donors are identical in CdTe and ZnTe. Results from a recent calculation show that CdTe/ZnTe (100) superlattices have a small valence-band offset of 0.1–0.3 eV.²⁶ Thus we expect that, because of the larger band gap of ZnTe, its conduction-band edge should be 0.5–0.7 eV higher in energy in CdTe. This is consistent with the larger binding energy of *DX* centers in ZnTe.

In order to examine the alloy dependence of the binding energies of *DX* centers in $\text{Cd}_{1-x}\text{Zn}_x\text{Te}$ alloys, we have calculated the *DX* binding energy for an In donor in the $x=0.5$ alloy. The result, as shown in Fig. 3, indicates that as the Zn ratio increases, the *DX* centers become stabilized compared with the d^0 state, and a shallow to deep transition is expected to occur at about $x=0.2$. If we assume a similar trend for the *DX* binding energy of Al, it is expected to undergo such a transition at about $x=0.8$. Thus *n*-type doping control in the alloys should be more easily achieved with Al impurities than with In.

Experimentally In donors in $\text{Cd}_{0.8}\text{Zn}_{0.2}\text{Te}$ alloy are nearly completely self-compensated by *DX* centers.⁴ Khachatryan *et al.* estimated the electron emission barrier from the *DX* centers to be 0.29 eV.⁴ In our calculation for In in $\text{Cd}_{0.8}\text{Zn}_{0.2}\text{Te}$, the thermal barriers for electron emission and capture are found to be about 0.3 eV, in good agreement with the experimental values.⁴ Since the optical excitation energy is estimated to be about 0.95 eV (from the calculated *DX* level at 0.15 eV below midgap), a large Stokes shift between the optical and thermal excitation energies is expected with the broken-bond geometry. The large lattice relaxation leads to two paired electrons at this center, and an EPR inactive center, in agreement with experimental data.⁴ Persistent photoconductivity and photoinduced EPR (Ref. 4) can be easily explained by the existence of a thermal barrier for both electron capture and emission together with a much larger optical excitation energy.

B. Column VII donors

For column VII donors such as Cl, Br, and I atoms, we find *three* types of large lattice relaxations with trigonal symmetry which are either metastable or stable for a negatively charged state. The three structures are illustrated in Figs. 1(c)–1(e). For the *DX*₁ structure in Fig. 1(c), a donor atom and a nearest-neighbor Cd atom ($\text{Cd}_{[111]}$) are each pushed in opposite directions toward their respec-

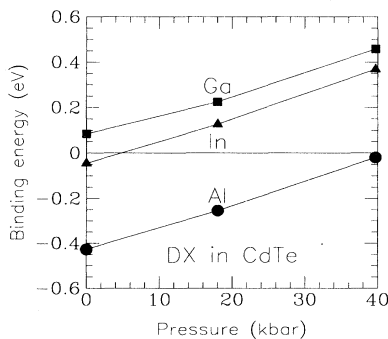


FIG. 4. The pressure dependence of the binding energies of *DX* centers for the column III donors In, Ga, and Al donors. They all have similar pressure derivatives of about 10.0 meV/kbar.

tive interstitial sites. This structure has the largest relaxation among the three structures. For the DX_2 structure in Fig. 1(d), the donor atom and the $Cd_{[111]}$ atom are both displaced along the $[111]$ direction. For the DX_3 structure in Fig. 1(e), the donor and $Cd_{[111]}$ atom are displaced together along the $[\bar{1}\bar{1}\bar{1}]$ direction. For the relaxed DX_1 , DX_2 , and DX_3 structures, the calculated Cl- $Cd_{[111]}$ separations are 5.50, 2.45, and 3.10 Å, respectively, while the other three donor-Cd bond lengths are 2.65, 2.77, and 2.61 Å, and these bonds make angles of 97.6°, 134.5°, and 84.6° with the axial direction. These bond lengths are smaller than the donor-Cd bond length of 2.83 Å calculated in the substitutional d^+ state.

The charge density contours for the three different DX -derived levels at the Γ point of the Brillouin zone are shown in Figs. 2(b)–2(d) for the Cl donor in CdTe. For DX_1 [Fig. 2(b)], the charge density is more localized around the $Cd_{[111]}$ atom than the donor atom. Away from the donor, the charge is more localized around the Te atoms, and has p character, due to the strong ionicity of CdTe. The charge localization in the DX_1 state is weak. For DX_2 and DX_3 [Figs. 2(c) and 2(d)], even though the separation between the Cl and $Cd_{[111]}$ atoms is reduced, the DX state becomes strongly localized around the donor atom. The energy levels of the localized states of DX_1 , DX_2 , and DX_3 for the Cl donor are calculated to be located at -0.22 , -0.47 , and -0.21 eV below the conduction-band minimum, respectively.

The calculated binding energies for Cl, Br, and I donors in CdTe and ZnTe for the DX_1 , DX_2 , and DX_3 structures are given in Table III. In CdTe all three DX centers are higher in energy than the shallow donor state. Among the three DX states, the DX_3 structure is the most stable state for Cl and Br donors, while the DX_1 structure is the most stable state for the I donor. In contrast, for ZnTe all three DX centers are more stable than the shallow donor state. The DX_3 structure is the most stable state for Cl, and the DX_1 structure is the most stable state for Br and I. Extension of the results to $Cd_xTe_{1-x}Te$ suggests that, for Br, DX_1 is more stable than either DX_3 or the shallow donor state. The DX_2 structure is not found to be a stable or metastable state for Br or I donors in either CdTe or ZnTe. However, as discussed next, DX_2 becomes stable at sufficiently high pressures. From the results of our calculations we note that for Cl in CdTe, the barriers from DX_2 or DX_3 to D^- are small, but with increasing pressure, the barriers be-

come larger. For an I donor, the large atomic size of the donor makes the energy of the DX_3 structure large relative to DX_1 .

Overall, these column VII donors give more stable shallow donor states than In or Ga donors (but not Al). Our results are in agreement with the recent demonstration⁷ that Cl and Br donors can easily give electron concentrations of $(2-3) \times 10^{18}/\text{cm}^{-3}$.

The pressure dependence of the binding energies for the three types of DX structures for the Cl donor is shown in Fig. 5. The pressure derivatives of the binding energies for the DX_2 and DX_3 structures are calculated to be about 14.5 and 8.3 meV/kbar, respectively. The binding energy of the DX_1 structure has a small negative pressure coefficient, which is due to the weak localized character of this DX state. It is worthwhile to note that at high pressure DX_2 becomes more stable than DX_3 . This can be explained by the increase in the energy of the DX_3 structure caused by the increased repulsive interaction between Cl and second-nearest-neighbor Te atoms. The calculated pressure derivatives for DX_2 binding energies for column VII donors are about 1.37 times larger than those for column III donors, in very good agreement with experimental observations.⁹ We suggest therefore that the DX centers observed at high pressure should have the DX_2 , rather than the DX_1 structure which is more stable at zero pressure. For Br and I donors, the DX_2 structure is not found to be the stable state in CdTe, but with increasing pressure, this structure can exist as a metastable or a stable state. The DX_2 state is predicted to become more stable than the DX_3 state around 23 and 28 kbar for Br and I, respectively. For Cl, such a stability change occurs at around 11 kbar. The pressure dependences of the DX binding energies for Br and I donors are similar to that of Cl.

The shallow-deep transitions are estimated to occur at pressures of about 14, 34, and 40 kbar for Cl, Br, and I donors, respectively. In our LDA calculation, the theoretical volume at zero pressure is underestimated (it is the volume one gets experimentally at 14 kbar). If we use the theoretical volume, the shallow-deep transition pressure is expected to occur at 0, 20, and 26 kbar for Cl, Br, and I donors, respectively. Experimentally such transitions were observed at 0–2 kbar for Cl, and at 10 kbar for Br. For I donor, it was not observed up to a pressure of 18 kbar.

We did not perform calculations of DX binding ener-

TABLE III. The binding energies in eV of the DX_1 , DX_2 , and DX_3 centers (shown in Fig. 1) for Cl, Br, and I donors in CdTe and ZnTe semiconductors. Negative values indicate that the shallow donor state is more stable than the DX center.

		Cl	Br	I
CdTe	DX_1	-0.32	-0.31	-0.16
	DX_2	-0.20		
	DX_3	-0.11	-0.16	-0.82
ZnTe	DX_1	0.09	0.15	0.39
	DX_2	-0.02		
	DX_3	0.17	-0.02	-2.97

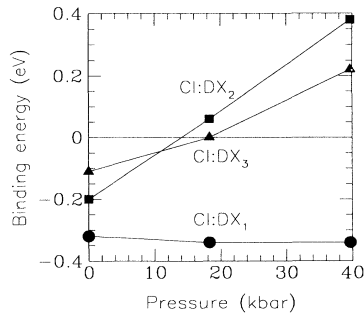


FIG. 5. The pressure dependence of the binding energies of the DX_1 , DX_2 , and DX_3 centers for a Cl donor. The DX_2 center has a large pressure derivative of 14.2 meV/kbar.

gies in $Cd_{1-x}Zn_xTe$ alloys, but we expect results similar to those shown in Fig. 3, i.e., that the addition of Zn to CdTe should make the DX_3 center of Cl stable with respect to the shallow donor state. The DX_2 structure is less stable than the DX_3 in $Cd_{1-x}Zn_xTe$ alloys, i.e., the DX_3 structure should play the role of the DX center in the Cl-doped alloys. The shallow to deep transition is expected to occur as before at a value of $x=0.4$. Experimentally, $Cd_{1-x}Zn_xTe$ alloys with $x=0.2$ or with even lower values of x exhibit DX centers.⁴ Our predicted transition ratio x is larger, but the present large lattice relaxation model explains well the shallow-deep transition through the addition of Zn to CdTe.

The fact that DX centers are observed even with very small additions of Zn to CdTe may be due to segregation in $Cd_{1-x}Zn_xTe$ alloys, i.e., the DX center can form in regions with higher Zn content. Generally the formation enthalpy for the alloys from the binary compounds is positive, which means the alloys are energetically unstable with respect to segregation. Jiang and Lin observed

the PPC effect in nominally undoped $Cd_{0.7}Zn_{0.3}Te$ and $CdSe_{0.5}S_{0.5}$ alloys, which they attributed to compositional inhomogeneities.²⁷ Since the DX center is calculated to be stable for a Cl donor in ZnTe, the possibility that compositional variations give rise to DX centers seems reasonable.

IV. CONCLUSIONS

We have performed first-principles total-energy calculations in order to examine the “negative- U ” large lattice relaxation model for column III and VII donors in CdTe, ZnTe, and $Cd_xZn_{1-x}Te$ alloys, and find that deep donor centers in these semiconductors are well explained by this model. Only Ga is found to give rise to a stable DX center in CdTe whereas in ZnTe all the donor impurities examined give deep centers. The theoretical results for pressure and alloy dependence in $Cd_xZn_{1-x}Te$ alloys are in good agreement with experimental data. Three types of DX centers are suggested for column VII donors. The DX_2 [Fig. 1(d)] structure becomes stable at high pressure, while in the alloys, the DX_1 [Fig. 1(c)] or DX_3 [Fig. 1(e)] structures are more stable than DX_2 . From our calculations, Al, Br, and I donors are suggested to be the best shallow donors in $Cd_xZn_{1-x}Te$ alloys with respect to compensation by DX centers.

More recently, we have found a new type of very low-energy lattice instability which is very effective in acceptor compensation in II-VI semiconductors.²⁸ We find that a similar type of lattice instability can give rise to donor passivation, especially for column VII impurities in II-VI semiconductors. The instability involves the rupture of two host bonds and the formation of a cation-cation dimer bond. The defect is a negative- U center and for the case of halogen dopants it provides a very effective compensation mechanism. More work is currently in progress to characterize this new defect.

¹S. Scholl, J. Gerschütz, H. Schäfer, F. Fischer, A. Waag, and G. Landwehr, *Solid State Commun.* **91**, 491 (1994).

²A. Waag, F. Fischer, J. Gerschütz, S. Scholl, and G. Landwehr, *J. Appl. Phys.* **75**, 1368 (1994).

³B. C. Burke, R. P. Khosla, J. R. Fischer, and D. L. Losee, *J. Appl. Phys.* **47**, 1095 (1976).

⁴K. Khachatryan, M. Kaminska, E. R. Weber, P. Becla, and R. A. Street, *Phys. Rev. B* **40**, 6304 (1989).

⁵I. Terry, T. Penney, S. von Molnár, J. M. Rigotty, and P. Becla, *Solid State Commun.* **84**, 235 (1992); I. Terry, S. von Molnár, A. M. Torrsen, and P. Becla, *Philos. Mag. B* **65**, 1245 (1992).

⁶F. Bassani, S. Tatarenko, K. Saminadayar, N. Magnea, R. T. Cox, A. Tardot, and C. Grattapain, *J. Appl. Phys.* **72**, 2927 (1992); F. Bassani, S. Tatarenko, K. Shaminadayar, J. Bleuse, N. Magnea, and J. L. Paultrat, *Appl. Phys. Lett.* **58**, 2651 (1991).

⁷A. Waag, Th. Litz, F. Fischer, H. Heinke, S. Scholl, D. Hommel, G. Landwehr, and G. Bilger, *J. Cryst. Growth* **138**, 437 (1994); D. Hommel, A. Waag, S. Scholl, and G. Landwehr, *Appl. Phys. Lett.* **61**, 1546 (1992).

⁸P. M. Mooney, *J. Appl. Phys.* **67**, R1 (1990).

⁹G. W. Iseler, J. A. Kafalas, A. J. Strauss, H. F. MacMillan, and R. H. Bube, *Solid State Commun.* **10**, 619 (1972).

¹⁰D. J. Chadi and K. J. Chang, *Phys. Rev. Lett.* **61**, 873 (1988); *Phys. Rev. B* **39**, 10063 (1989); D. J. Chadi, *Phys. Rev. Lett.* **72**, 534 (1994).

¹¹D. J. Chadi, *Annu. Rev. Mater. Sci.* **24**, 45 (1994).

¹²H. P. Hjalmarson, P. Vogl, D. J. Wolford, and J. D. Dow, *Phys. Rev. Lett.* **44**, 810 (1980).

¹³J. D. Dow, O. F. Sankey, and R. V. Kasoowski, *Phys. Rev. B* **43**, 4396 (1991).

¹⁴M. L. Cohen, *Phys. Scr.* **T1**, 5 (1982).

¹⁵P. Hohenberg and W. Kohn, *Phys. Rev.* **136**, B864 (1964); W. Kohn and L. J. Sham, *ibid.* **140**, A1133 (1965).

¹⁶J. Ihm, A. Zunger, and M. L. Cohen, *J. Phys. C* **12**, 4409 (1979).

¹⁷N. Troullier and J. L. Martins, *Phys. Rev. B* **43**, 1993 (1991).

¹⁸L. Kleinman and D. M. Bylander, *Phys. Rev. Lett.* **48**, 1424 (1982).

¹⁹G. B. Bachelet and M. Schlüter, *Phys. Rev. B* **25**, 2103 (1982); L. Kleinman, *ibid.* **21**, 2630 (1980).

²⁰P. M. Ceperly and B. J. Alder, *Phys. Rev. Lett.* **45**, 566 (1980); J. P. Perdew and A. Zunger, *Phys. Rev. B* **23**, 5048 (1981).

- ²¹S. G. Louie, S. Froyen, and M. L. Cohen, *Phys. Rev. B* **26**, 1738 (1982).
- ²²S. B. Zhang and D. J. Chadi, *Phys. Rev. B* **42**, 7174 (1990).
- ²³B. H. Cheong and K. J. Chang, *Phys. Rev. B* **46**, 13 131 (1992).
- ²⁴B. H. Cheong and K. J. Chang, *Phys. Rev. Lett.* **71**, 4354 (1993).
- ²⁵A. G. Foyt, R. E. Halsted, and W. Paul, *Phys. Rev. Lett.* **16**, 55 (1966).
- ²⁶A. Continenza and S. Massidda, *Phys. Rev. B* **50**, 11 949 (1994).
- ²⁷H. X. Jiang and J. Y. Lin, *Phys. Rev. Lett.* **64**, 2547 (1990); H. X. Jiang and J. Y. Lin, *Phys. Rev. B* **41**, 5178 (1990).
- ²⁸C. H. Park and D. J. Chadi, *Phys. Rev. Lett.* **75**, 1134 (1995).